



Title	Integrating multiple scan matching results for ego-motion estimation with uncertainty
Author(s)	Koyasu, Hiroshi; Miura, Jun; Shirai, Yoshiaki
Citation	2004 IEEE/RSJ International Conference on Intelligent Robots and Systems (IROS). 2004, 3, p. 3104-3109
Version Type	VoR
URL	<a href="https://hdl.handle.net/11094/14094">https://hdl.handle.net/11094/14094</a>
rights	c2004 IEEE. Personal use of this material is permitted. However, permission to reprint/republish this material for advertising or promotional purposes or for creating new collective works for resale or redistribution to servers or lists, or to reuse any copyrighted component of this work in other works must be obtained from the IEEE..
Note	

*The University of Osaka Institutional Knowledge Archive : OUKA*

<https://ir.library.osaka-u.ac.jp/>

The University of Osaka

# Integrating Multiple Scan Matching Results for Ego-Motion Estimation with Uncertainty

Hiroshi Koyasu, Jun Miura, and Yoshiaki Shirai  
Department of Computer-Controlled Mechanical Systems, Osaka University  
Email: {koyasu,jun,shirai}@cv.mech.eng.osaka-u.ac.jp

**Abstract**—This paper describes an ego-motion estimation method by integrating multiple scan matching results. The method considers both the uncertainty of scan matching results and that of estimated ego-motions, and not only estimates the latest ego-motion but also updates previous ego-motions. The estimation process is formulated as an iterative one using Kalman filter. We implement the method by using an omnidirectional stereo-based scan matching method. Experimental results show the effectiveness of the proposed method.

## I. INTRODUCTION

Reliable ego-motion estimation is indispensable for integrating sensing data which are obtained by a moving observer. Since dead reckoning suffers from accumulated errors, an ego-motion estimation method is needed which is based on external sensors such as vision. Scan matching-based methods (e.g., [9]), which do not need explicit feature correspondence, have an advantage over feature-based methods (e.g., [2], [3]), which may require much computation in extracting stable features and in finding correct matches.

Lu et al. [9] estimated the ego-motion by comparing 2D contours obtained by a laser range finder at the current and the previous position. Pfister et al. [11] extended their method to consider the uncertainty of the estimated ego-motion in order to integrate the scan matching-based ego-motion with odometry information. Since these methods use only a pair of laser scans, sensor noises may cause wrong matches thereby degrading estimation results. Kidono et al. [6] proposed a scan matching-based localization method, which compares the current range scan with the range scan predicted from the generated map; their method, however, did not consider the uncertainty in localization. Hähnel et al. [4] considered the uncertainty in a similar scan matching method; once a robot position is estimated, however, it is not changed by subsequent observations.

Scans may sometimes include large uncertainties, especially when using low-precision range sensors such as stereo, and an ego-motion or a robot position obtained using these scans may thus be unreliable. We, therefore, must be able to update previously-estimated ego-motions or robot positions, if necessary. In simultaneously localization and mapping (SLAM) problems, some research re-estimates ego-motion to close loops (e.g., [1], [5]); but the re-estimation is limited to the timing of closing the loop.

This paper deals with ego-motion estimation from multiple scan matching results. Fig. 1 shows an example situation where a robot obtains three range scans at times  $t - 2$ ,  $t - 1$ , and  $t$ . Let  $X_t^{(t-1)}$  be the ego-motion during

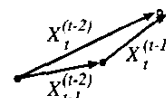


Fig. 1. Integrate tree scan matching results.

$[t - 1, t]$ ; it can be calculated by comparing two scans at time  $t - 1$  and  $t$ . Similarly, we obtain  $X_{t-1}^{(t-2)}$ . This is basically what the previous methods are doing which use only a pair of range scans for ego-motion estimation. We can, however, use the other scan matching result,  $X_t^{(t-2)}$ , to improve the ego-motion estimation. This is the basic idea of our method.

Our previous work [8] has already dealt with ego-motion estimation using multiple scan matching results. Although the method outperformed previous methods which use only a pair of scans for estimating an ego-motion, it still had the following two drawbacks. One is that at each time, only the latest ego-motion is estimated with believing the previous ego-motion estimates; so if some of previous estimates are unreliable, the current estimate becomes inherently unreliable too. The other drawback is that all scan matching results are treated evenly; the estimation result may be degraded by matching results with large uncertainties.

This paper improves our previous method so that we can simultaneously estimate the current and the previous ego-motions with considering the uncertainty of each scan matching result. Estimating  $k$  ego-motions from scratch needs to examine  ${}_{k+1}C_2$  pairs of range scans, and this may be costly. We therefore develop a Kalman filter-based iterative scheme which estimates the current ego-motion and updates the previous  $k - 1$  ego-motions simultaneously by using only  $k + 1$  newly obtained scan matching results.

The rest of this paper is organized as follows. Section II describes the ego-motion estimation algorithm by using multiple scan matching results. Section III describes an implementation of the method using an omnidirectional stereo. Section IV shows experimental results using a real robot. Section V summarizes the paper.

## II. PROPOSED ALGORITHM

This section describes a Kalman filter-based algorithm of integrating multiple scan matching results for ego-motion estimation. Basically we use the latest  $k + 1$  range scans for estimating  $k$  ego-motions. Actually, our method estimates the relative position of latest  $k$  observation points (including the current one) with respect to the observation point  $k$  steps before.

Let  $X_{t-i}^{(t-k)} = (x_{t-i}^{(t-k)}, y_{t-i}^{(t-k)}, \theta_{t-i}^{(t-k)})^T$  denote the relative position at time  $t - i$  with respect to the position at time

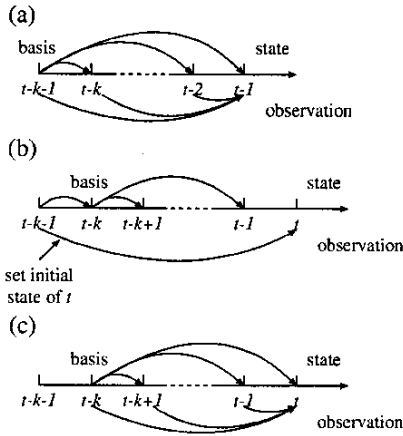


Fig. 2. State transition model.

$t - k$ . The state  $S_t$  is represented by the vector:

$$S_t = \left( X_{t-k+1}^{(t-k)T}, X_{t-k+2}^{(t-k)T}, \dots, X_t^{(t-k)T} \right)^T. \quad (1)$$

An observation is a set of  $k$  scan matching results between the current and the previous  $k$  range data. Let  $p_{t,t-i}$  denote the scan matching result (i.e., the observed relative displacement) obtained by range scans at time  $t$  and  $t - i$ . Then the observation is represented by the vector:

$$P_t = (p_{t,t-k}^T, p_{t,t-k+1}^T, \dots, p_{t,t-1}^T)^T. \quad (2)$$

Fig. 2 illustrates the iteration process. Fig. 2(a) shows the situation where the relative position at times  $t - k$  to  $t - 1$  with respect to the position at time  $t - k - 1$  are estimated using the observations until time  $t - 1$ . Fig. 2(b) shows the state transition from  $S_{t-1}$  to  $S_t$ ; the relative position at time  $t$  with respect to a new basis (position at time  $t - k$ ) is calculated from the difference between a relative position,  $X_{t-k}^{t-k-1}$ , in  $S_{t-1}$  and the scan matching result between range data at time  $t$  and  $t - k - 1$ . Fig. 2(c) indicates the estimation of  $S_t$  by integrating new  $k$  scan matching results.

The state transition equation (see Fig. 2(b)) is given by:

$$S_{t,t-1} = \begin{pmatrix} -I & I & \dots & 0 \\ \vdots & \vdots & \ddots & \vdots \\ -I & 0 & \dots & I \\ 0 & 0 & \dots & 0 \end{pmatrix} S_{t-1,t-1} + \begin{pmatrix} 0 \\ \vdots \\ 0 \\ p_{t,t-k-1} \\ -X_{t-k}^{(t-k-1)} \end{pmatrix} + v_t \quad (3)$$

$$v_t = \begin{pmatrix} 0 \\ \vdots \\ 0 \\ \delta p_{t,t-k-1} - \delta X_{t-k}^{(t-k-1)} \end{pmatrix},$$

where  $\delta p_{t,t-k-1}$  and  $\delta X_{t-k}^{(t-k-1)}$  are the errors of the observation  $p_{t,t-k-1}$  and the relative position vector  $X_{t-k}^{(t-k-1)}$  respectively. In this equation, the initial value of  $X_t^{(t-k)}$  is estimated from  $p_{t,t-k-1}$  and  $X_{t-k}^{(t-k-1)}$ ; this means that our Kalman filter integrates only observations. It is a simple extension to integrate odometry information into this formulation.

The observation equation (see Fig. 2(c)) is given by:

$$P_t = \left( \begin{array}{ccc|c} 0 & \dots & 0 & I \\ -I & \dots & 0 & I \\ \vdots & \ddots & \vdots & \vdots \\ 0 & \dots & -I & I \end{array} \right) S_t + w_t, \quad (4)$$

where  $w_t$  is a noise vector,  $0$  is  $3 \times 3$  dimensional zero matrix, and  $I$  is 3-dimensional unit matrix.

A scan is composed of a set of observed points. So the error of a scan matching result  $p_{t,t-i}$  is caused by two factors: the observation error of the points and false correspondence between the points. Since every scan matching result in eq. (2) uses the same observation at time  $t$ , the errors of these scan matching results are not independent. However, since the number of points in a scan is usually large, the influence of an observation error to the scan matching error is considered sufficiently smaller than that of false correspondence, which depends on the shape of the surrounding environment. Thus we assume that the errors of scan matching results in eq. (2) are mutually independent. Under this assumption, the covariance matrix of  $w_t$  is calculated by:

$$\Sigma_{P_t} = \begin{pmatrix} \Sigma_{p_{t,k}} & 0 & \dots & 0 \\ 0 & \Sigma_{p_{t,k+1}} & \dots & 0 \\ \vdots & \vdots & \ddots & \vdots \\ 0 & \dots & 0 & \Sigma_{p_{t-1}} \end{pmatrix}, \quad (5)$$

where  $\Sigma_{p_{t,i}}$  is calculated as the uncertainty of the corresponding scan matching result (see Sec. III-D).

By applying Kalman filter to eqs. (3) and (4), we iteratively update the state  $S_t$  and estimate its uncertainty. At the initial position, the robot position and orientation are considered to have no uncertainty. We use 5 as  $k$ , and if the number of observations is less than  $k + 1$ , we set the dimension of the state vector accordingly.

### III. OMNIDIRECTIONAL STEREO-BASED SCAN MATCHING

This section describes an implementation of the ego-motion estimation method using an omnidirectional stereo. To apply the ego-motion estimation method, we need a scan matching method which not only calculate the relative position between observation points but also its uncertainty.

The outline of the scan matching method is as follows. We first compute the uncertainty of the current robot position (with respect to some basis position) calculated by dead reckoning to determine a set of possible robot positions and orientations. Next, we calculate the difference between the views of the current and the previous range data for each candidate pair of the position and the orientation, and estimate the reliability of each candidate. Finally, we determine the current position and orientation with their uncertainties by a weighted least squares-based estimation.

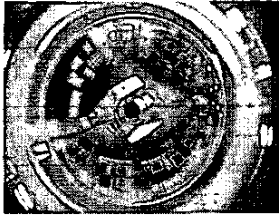


Fig. 3. An example of the original input image.



Fig. 4. Panoramic image obtained from the input image shown in Fig. 3.



Fig. 5. Panoramic disparity image obtained from the images in Fig. 4. Brighter pixels are nearer.

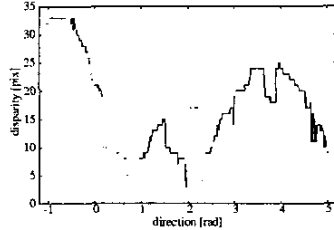


Fig. 6. Example range profile.

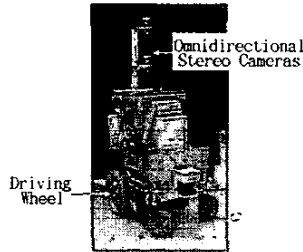


Fig. 7. Our mobile robot.

### A. Omnidirectional Stereo

Our scan matching method uses the omnidirectional stereo. The omnidirectional stereo vision system uses two HyperOmni Vision [13] aligned vertically. Fig. 3 shows an input image of the lower camera of our stereo system. Each image can be converted to a panoramic image shown in Fig. 4 by projecting on a cylindrical image plane whose axis is aligned to an optical axis of the camera. By this conversion, we can obtain a stereo image pair where all epipolar lines become vertical. Therefore, we can apply a conventional stereo matching algorithm for an ordinary perspective stereo. We use an SAD-based stereo matching algorithm. For the detail of this omnidirectional stereo, refer to [7].

To adopt a visual ego-motion estimation method, we first extract the nearest obstacle in each direction. Since the horizontal axis of the panoramic image indicates the horizontal direction, we extract the nearest obstacles in every column, then we obtain a set of disparities of about 360 degrees. From this data set, a 2D contour (called *range profile (RP)*) of the current free space centered at the robot position is obtained. Fig. 6 shows the RP obtained from the disparity image shown in Fig. 5. In Fig. 6, the horizontal axis represents the viewing direction from the robot and the vertical axis represents disparity of obstacles.

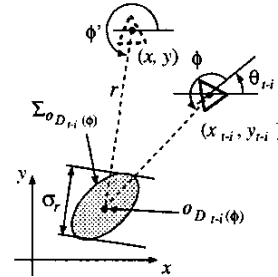


Fig. 8. View of previous observed obstacle from candidate position.

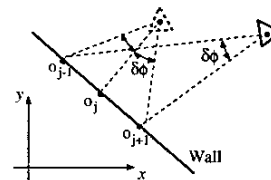
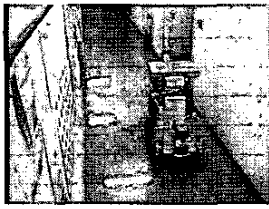


Fig. 9. Problem caused by fixed angular resolution.

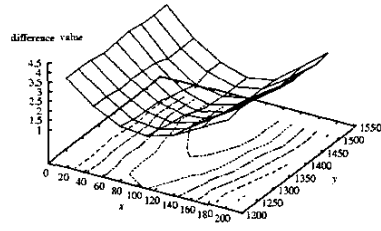
### B. Select Candidate Positions and Orientations

Fig. 7 shows our mobile robot. The robot moves by driving the two rear wheels. We define a state of the robot as  $\mathbf{X} = (x, y, \theta)$ , where  $(x, y)$  is a 2-dimensional robot position centered at the omnidirectional stereo cameras,  $\theta$  is an orientation of the robot. The positional uncertainty increases as the robot moves due to slippage of wheels or a quantization error of odometry. We model the uncertainty by a three-dimensional normal distribution; the so-called  $3\sigma$  ellipsoid obtained from the covariance matrix  $\Sigma_{\mathbf{X}_t}$  represents the uncertainty region. The positional uncertainty on  $(x, y)$  is calculated by projecting the ellipsoid on the  $x$ - $y$  plane and the orientational uncertainty is calculated as its marginal distribution on  $\theta$ .

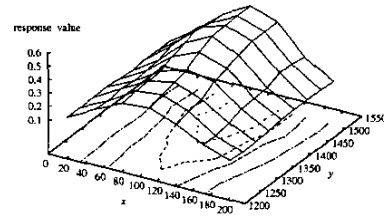
We select candidates of robot position and orientation in the region. Candidates of the position are set at lattice points which are made by lines parallel with two principal axes of the ellipse. The origin of the lattice is set at the center of the ellipse. The number of lattice points along each axis is selected as the minimum odd number greater than 3, by which the length of the principal axis divided is smaller than  $50[mm]$ . For example, when the length of the longer principal axis is  $200[mm]$  and that of the shorter is  $140[mm]$ , the number of the candidate positions becomes  $5 \times 3$ . Candidates for the robot orientation are generated by discretizing the range of the orientational uncertainty with the angular resolution of the RP.



(a) experimental environment



(b) difference values



(c) estimated probability distribution

Fig. 10. Estimation of the positional distribution.

### C. Comparing Two Range Profiles

To compare the current and a previous RP, we predict the view of the previous RP for each candidate position and orientation. Fig. 8 indicates the situation where the robot at candidate position  $(x, y)$  is observing an object which was observed at position  $\mathbf{X}_{t-i} = (x_{t-i}, y_{t-i}, \theta_{t-i})$ . We would like to predict the direction and the disparity of the object in order to predict the view of a previous RP. The obstacle position  $\mathcal{O}_{D_{t-i}(\phi)}$ , which is observed at time  $t-i$  in direction  $\phi$  with disparity  $D_{t-i}(\phi)$ , is represented by using the robot position  $\mathbf{X}_{t-i}$ :

$$\mathcal{O}_{D_{t-i}(\phi)} = \begin{pmatrix} \frac{bf}{D_{t-i}(\phi)} \cos(\theta_{t-i} + \phi) + x_{t-i} \\ \frac{bf}{D_{t-i}(\phi)} \sin(\theta_{t-i} + \phi) + y_{t-i} \end{pmatrix}, \quad (6)$$

where  $b$  represents the baseline of the omnidirectional stereo, and  $f$  represents the focus length of panoramic images.  $\Sigma_{\mathcal{O}_{D_{t-i}(\phi)}}$ , which is the error covariance matrix of  $\mathcal{O}_{D_{t-i}(\phi)}$ , is calculated from  $\Sigma_{\mathbf{X}_{t-i}}$ , which is the error covariance matrix of the position  $\mathbf{X}_{t-i}$ , and  $\sigma_{D_{t-i}(\phi)}^2$ , which is the error variance of disparity  $D_{t-i}(\phi)$ , by error propagation. We set  $\sigma_{D_{t-i}(\phi)}^2 = \sigma_{D^*}^2 = 1$  as the quantization error of panoramic images.

Once  $\mathcal{O}_{D_{t-i}(\phi)}$  is calculated, we can determine the relative position of  $\mathcal{O}_{D_{t-i}(\phi)}$  from a candidate position  $(x, y)$ , and then we can calculate the distance  $r$  and the direction  $\phi'$  to  $\mathcal{O}_{D_{t-i}(\phi)}$  from the candidate position. By converting the distance  $r$  to the disparity by using the relation  $D = \frac{bf}{r}$ , we can calculate  $D_{t-i}^{(x,y)}(\phi')$  which is the disparity of the obstacle  $\mathcal{O}_{D_{t-i}(\phi)}$  viewed from a candidate position  $(x, y)$ . Also  $\sigma_{D_{t-i}^{(x,y)}(\phi')}^2$ , which is the error variance of  $D_{t-i}^{(x,y)}(\phi')$ , is calculated from  $\Sigma_{\mathcal{O}_{D_{t-i}(\phi)}}$  by error propagation.

The prediction of the view of a previous RP is performed by converting each observed disparity in the previous RP to the disparity to be observed from a candidate position. There is, however, a possibility that such converted disparities are not obtained for several directions in the predicted RP, due to the fixed angular resolution. Fig. 9 shows the situation where the disparity corresponding to the  $j$ th direction has not been obtained in the previous observation. In such cases, if the nearest disparities on the both sides (e.g.,  $o_{j-1}$  and  $o_{j+1}$  in the figure) are close enough to be regarded to belong to the same obstacle, the disparity in the  $j$ th direction is calculated by linearly interpolating the object surface from the disparities of  $o_{j-1}$  and  $o_{j+1}$ .

We obtain the predicted view from candidate position  $(x, y)$  of an RP obtained at  $t-i$  by applying the above

calculation to all disparities in the RP. In a candidate position and orientation  $(x, y, \theta)$ , the difference of the disparities in direction  $\phi$  of the current RP and the RP observed at time  $t-i$  is calculated by:

$$d(x, y, \theta, i, \phi) = \frac{(D_t(\phi) - D_{t-i}^{(x,y)}(\phi - \theta))^2}{\sigma_{D^*}^2 + \sigma_{D_{t-i}^{(x,y)}(\phi - \theta)}^2}, \quad (7)$$

where  $D_t(\phi)$  represents the disparity in direction  $\phi$  at time  $t$ .  $d(x, y, \theta, i, \phi)$  represents the Mahalanobis distance; if the two disparity values in eq. (7) are from the same obstacle,  $d$  is assumed to follow a  $\chi^2$  distribution. Therefore, when  $d$  is larger than a certain threshold determined from  $3\sigma$  value of the  $\chi^2$  distribution,  $d$  is set as the threshold value. Also, when  $D_t(\phi)$  or  $D_{t-i}^{(x,y)}(\phi - \theta)$  is not obtained, we do not calculate the difference in that direction. By limiting the maximum difference by considering the  $\chi^2$  distribution, the effect of false matches in stereo and that of the moving obstacles can be reduced.

The difference of RPs is then evaluated by:

$$Diff(x, y, \theta, i) = \frac{1}{N(x, y, \theta, i)} \sum_{\phi=\phi_{min}}^{\phi_{max}} d(x, y, \theta, i, \phi), \quad (8)$$

where  $[\phi_{min}, \phi_{max}]$  represents the range of possible viewing directions (corresponding to the right and the left end of panoramic image);  $N(x, y, \theta, i)$  indicates the number of data for which the difference of disparity is obtained.

### D. Estimating Ego-Motion

Fig. 10(b) shows an example distribution of difference values  $Diff$  around the predicted position in a corridor shown in Fig. 10(a). From this figure, we can consider that the correct robot position lies in the valley of the distribution, and that the shape of this valley is related to the probability distribution of the robot position. So we would like to obtain the probability distribution of the robot position and orientation from the difference distribution.

Nickels and Hutchinson [10] solved a similar problem of estimating the uncertainty of the target localization in a template-based tracking. They calculate the distribution of the SSD values between a template image and an image region around the predicted position. They consider that the shape of the valley of this distribution represents the uncertainty of the target localization, just like us. Then, they convert the distribution of the SSD to *response distribution*, which is defined by Singh and Allen [12]. The response distribution calculates the confidence of each estimated position.

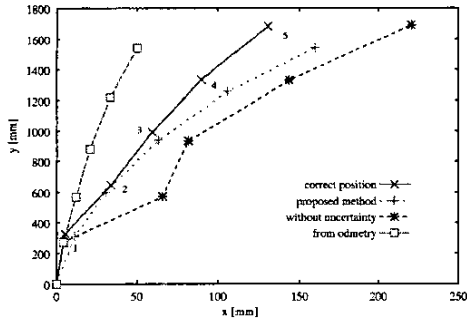


Fig. 11. Results of the experiment in section IV-A.

In our method, the response distribution is represented by the following:

$$r(x, y, \theta, i) = \exp(-\kappa \text{Diff}(x, y, \theta, i)), \quad (9)$$

where  $\kappa$  is used as a normalization factor. We set  $\kappa = 1$  experimentally. Fig. 10(c) shows the response distribution converted from Fig. 10(b).

Since the response distribution can be interpreted as a probability distribution of the position and orientation, we approximate the distribution by a 3D Gaussian. The mean of the Gaussian is calculated by a weighted least squares as:

$$\hat{x}_i = \frac{\sum_{x,y,\theta} r(x,y,\theta,i)x}{\sum_{x,y,\theta} r(x,y,\theta,i)}, \quad \hat{y}_i = \frac{\sum_{x,y,\theta} r(x,y,\theta,i)y}{\sum_{x,y,\theta} r(x,y,\theta,i)}, \quad (10)$$

$$\hat{\theta}_i = \frac{\sum_{x,y,\theta} r(x,y,\theta,i)\theta}{\sum_{x,y,\theta} r(x,y,\theta,i)}.$$

The covariance matrix can be calculated accordingly.

The ego-motion estimation method described in Sec. II requires scan matching results  $\mathbf{p}_{t,t-i}$  and their uncertainties  $\Sigma_{\mathbf{p}_{t,t-i}}$ . We use  $(\hat{x}_i, \hat{y}_i, \hat{\theta}_i)$  as  $\mathbf{p}_{t,t-i}$  and its covariance matrix as  $\Sigma_{\mathbf{p}_{t,t-i}}$ .

## IV. EXPERIMENTS

### A. Effect of Estimating Uncertainty

The experiment was done in the corridor environment shown in Fig. 10(a). In the experiment, the robot moved straight, and we gave an error for odometry data intentionally by making the robot go over the cord. Due to the effect of the error, the final position of the robot was at  $(140, 1600)[mm]$ .

We compared the proposed method with one of our previous methods [7], which selects the position and the orientation minimizing the sum of the differences between the current and the 5 previous RPs, dead reckoning by odometry, and the correct trajectory obtained by measuring the actual robot positions.

Fig. 11 shows the correct and the estimated robot trajectories. In estimating the position numbered 2 in the figure, our previous method (denoted as “without uncertainty”) selected position  $(66, 571)$ , where the minimum difference is 1.02596, while at the lattice point  $(20, 568)$  which is nearest to the correct position, the difference value is 1.14596. Since the difference distribution has a wide valley around the correct position, this result was caused by a small noise in range data. Since the previous method does

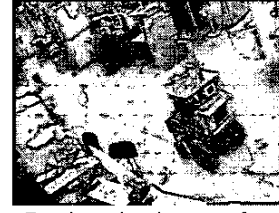


Fig. 12. Experimental environment of section IV-B.

TABLE I

ERROR OF THE EGO-MOTION ESTIMATION.

	x [mm]	y [mm]	$\theta$ [rad]
proposed method	147.03	107.07	0.17
method in [8]	173.44	139.88	0.23
method in [7]	274.42	156.5	0.18

not have a mechanism to correct such errors in subsequent estimations, the error grows relatively rapidly.

On the other hand, our proposed method estimated almost correct position for the  $x$  axis. While for the  $y$  axis, since there were not enough features to determine the robot  $y$  position, the error is relatively large, but the correct position was inside the estimated uncertainty region.

### B. Experiment in a Complex Environment

We conducted another experiment in a complex environment where many obstacles exist. For comparison, we show results which are estimated by two other method. One is the method which does not consider the uncertainty of the estimation described in the previous section. The other is the method proposed in [8], which estimates the position and orientation and its uncertainty from the distribution of the summation of differences between scan data, not evaluating the uncertainty of each scan matching result.

Fig. 12 shows the environment of this experiment. Figs. 13-15 show the error of the estimated ego-motion along the  $x$ , the  $y$ , and the  $\theta$  axes on the robot local coordinates, respectively. In these figures, the estimated uncertainties are also shown by error bars. Fig. 16 shows the correct trajectory (indicated as “correct position”) of the robot, and the trajectories which are calculated by accumulating the estimated ego-motions for the proposed method (“proposed method”), the method by [8] (“without Kalman filter”), and the method by [7] (“without uncertainty”). Table I shows the standard deviation of the error of  $x$ ,  $y$ , and  $\theta$  on the robot local coordinates shown in Figs. 13-15.

In these figures and the table, the estimations of the robot orientation are almost correct for all methods. The reason is probably that all methods use range data in various directions obtained from the omnidirectional stereo. About the estimation of the robot position, Fig. 16 and Table I shows that the proposed method performs best. Concerning the uncertainty estimates, Figs. 13-15 show that the correct ego-motions are almost always within the estimated uncertainties; this indicates the effectiveness of the proposed uncertainty estimation method. Only the last estimation of the orientation was not correct. This is because the robot motion was out of the uncertainty model of dead reckoning; this problem is expected to be solved by refining the uncertainty model.

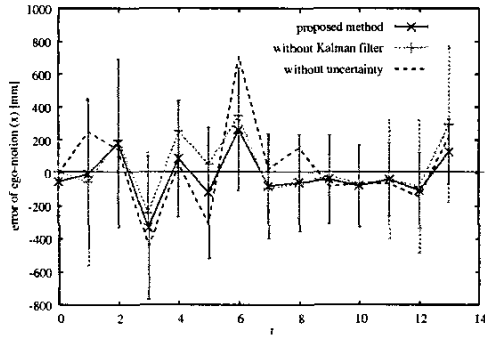


Fig. 13. Error of ego-motion of robot (x).

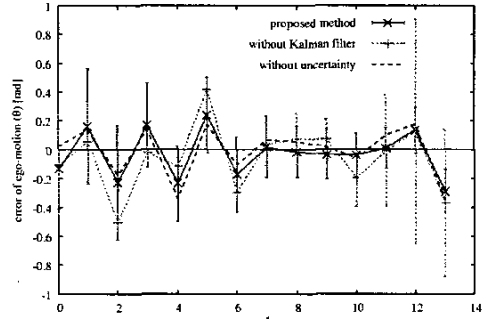


Fig. 15. Error of ego-motion of robot ( $\theta$ ).

#### V. CONCLUSION

This paper has proposed an ego-motion estimation method by integrating multiple scan matching results. The method simultaneously estimates the current and the previous ego-motions with considering the uncertainty of each scan matching result. Since the estimation process is formulated as an iterative one using Kalman filter, we can estimate the current ego-motion and update the previous  $k - 1$  ego-motions simultaneously by using only  $k + 1$  newly obtained scan matching results. We implement the method by using omnidirectional stereo-based scan matching method. Experimental result show the effectiveness of the proposed method.

Since the proposed method identifies false matches between range measurements using the Mahalanobis distance, it can be applied to dynamic environments where only a few moving objects exist. If there are many moving objects, however, the measurement from a moving object may match with that from another, and thus the ego-motion estimation may be degraded. A future work is, therefore, to develop a method of finding correct matches between the range measurements in a highly dynamic environment.

#### REFERENCES

- [1] H. Baltzakis and P. Trahanias. Closing Multiple Loops while Mapping Features in Cyclic Environments. In *Proc. of 2003 IEEE/RSJ Int. Conf. on Intelligent Robots and Systems*, pages 717–722, 2003.
- [2] G. Dissanayake, H. Durrant-Whyte, and T. Bailey. A Computationally Efficient Solution to the Simultaneous Localization and Map Building (SLAM) Problem. In *Proc. of IEEE Int. Conf. on Robotics and Automation*, pages 1009–1014, 2000.
- [3] M. Etoh, T. Aoki, and K. Hata. Estimation of Structure and Motion Parameters for a Roaming Robot that Scans the Space. In *Proc. of 7th Int. Conf. on Computer Vision*, volume 1, pages 579–584, 1999.

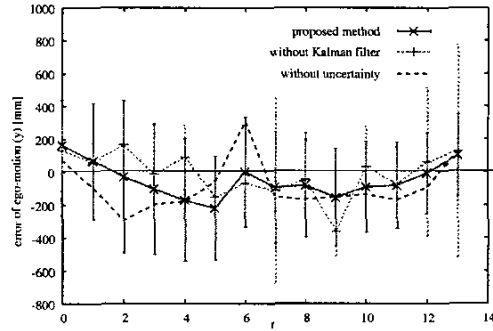


Fig. 14. Error of ego-motion of robot (y).

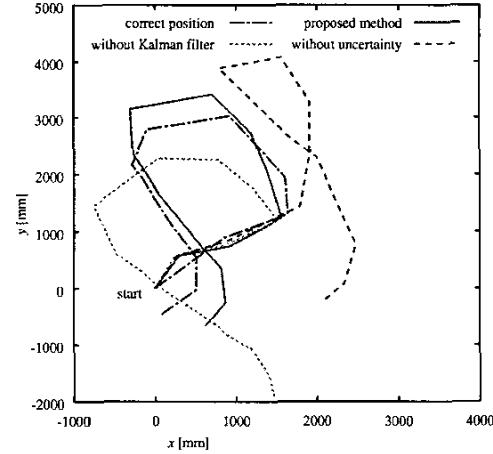


Fig. 16. Estimated position.

- [4] D. Hähnel, D. Schulz, and W. Burgard. Map Building with Mobile Robots in Populated Environments. In *Proc. of 2002 IEEE/RSJ Int. Conf. on Intelligent Robots and Systems*, pages 496–501, 2002.
- [5] D. Hähnel, D. Schulz, and W. Burgard. An Efficient FastSLAM Algorithm for Generating Maps of Large-Scale Cyclic Environments from Raw Laser Range Measurements. In *Proc. of 2003 IEEE/RSJ Int. Conf. on Intelligent Robots and Systems*, pages 206–211, 2003.
- [6] K. Kidono, J. Miura, and Y. Shirai. Autonomous Visual Navigation of a Mobile Robot Using a Human-Guided Experience. *Robotics and Autonomous Systems*, 40(2-3):121–130, 2002.
- [7] H. Koyasu, J. Miura, and Y. Shirai. Realtime Omnidirectional Stereo for Obstacle Detection and Tracking in Dynamic Environments. In *Proc. of IEEE Int. Conf. on Intelligent Robots and Systems*, pages 31–36, 2001.
- [8] H. Koyasu, J. Miura, and Y. Shirai. Mobile Robot Navigation in Dynamic Environments using Omnidirectional Stereo. In *Proc. of 2003 IEEE Int. Conf. on Robotics and Automation*, pages 893–898, 2003.
- [9] F. Lu and E. Milios. Robot Pose Estimation in Unknown Environments by matching 2D Range Scans. *Journal of Intelligent and Robotic Systems*, 18:249–275, 1997.
- [10] K. Nickels and S. Hutchinson. Estimating uncertainty in SSD-based feature tracking. *Image and Vision Computing*, 20:47–58, 2002.
- [11] S. T. Pfister, K. L. Kriechbaum, S. I. Roumeliotis, and J. W. Burdick. Weighted Range Sensor Matching Algorithms for Mobile Robot Displacement Estimation. In *Proc. of IEEE Int. Conf. on Robotics and Automation*, pages 1667–1674, 2002.
- [12] A. Singh and P. Allen. Image-Flow Computation: An Estimation-Theoretic Framework and a Unified Perspective. *Computer Vision Graphics and Image Processing: Image Understanding*, 56(2):152–177, 1992.
- [13] K. Yamazawa, Y. Yagi, and M. Yachida. Omnidirectional Imaging with Hyperboloidal Projection. In *Proc. of 1993 IEEE/RSJ Int. Conf. on Intelligent Robots and Systems*, pages 1029–1034, 1993.